THE JOURNAL OF PHYSICAL CHEMISTRY C

Article

Cite This: J. Phys. Chem. C XXXX, XXX, XXX–XXX

pubs.acs.org/JPCC

# Fast Energy Transfer in CdSe Quantum Dot Layered Structures: Controlling Coupling with Covalent-Bond Organic Linkers

Eyal Cohen,[†] Pavel Komm,[†] Noa Rosenthal-Strauss,[†] Joanna Dehnel,[∥] Efrat Lifshitz,[∥] Shira Yochelis,[†] Raphael D. Levine,[§] Francoise Remacle,[⊥] Barbara Fresch,[#] Gilad Marcus,[†] and Yossi Paltiel[†,‡,*]

[†]Department of Applied Physics, [‡]Center for Nano-Science and Nano-Technology, and [§]The Fritz Haber Center for Molecular Dynamics and Institute of Chemistry, The Hebrew University of Jerusalem, Jerusalem 9190401, Israel

[∥]Schulich Faculty of Chemistry, Solid State Institute and Rusell Berrie Nanotechnology Institute, Technion, Haifa 3200003, Israel

[⊥]Theoretical Physical Chemistry, UR MolSys, University of Liege, B4000 Liege, Belgium

[#]Department of Chemical Science, University of Padova, Via Marzolo 1, 35131 Padova, Italy

Supporting Information

**ABSTRACT:** Quantum dot (QD) solids and arrays hold a great potential for novel applications which are aimed at exploiting quantum properties in room-temperature devices. Careful tailoring of the QD energy levels and coupling between dots could lead to efficient energy-harvesting devices. Here, we used a self-assembly method to create a disordered layered structure of QDs, coupled by covalently bonded organic molecules. Energy transfer rates from small (donor) to large (acceptor) QDs are measured. Best tailoring of the QDs energy levels and the length of the linking molecules results in an energy transfer rate as high as 30 $ps^{-1}$. Such rates approach energy transfer rates of the highly efficient photosynthesis complexes and are compatible with a coherent mechanism of energy transfer. These results may pave way for new controllable building blocks for future technologies.

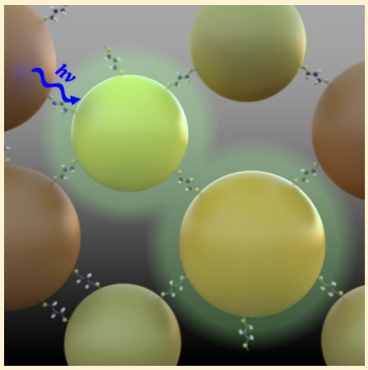


## INTRODUCTION

Semiconductor quantum dots (QDs) are known to exhibit optical and electrical characteristics which depends on their size, composition, and shape. When coupled in assemblies, they can be used as building blocks for "artificial molecules" or "artificial solids", which are expected to yield novel properties.[1−5] In turn, such new materials can be implemented in a variety of applicative uses, such as solar energy harvesting, sensing, light emission, and information processing.[6−15] For many such applications, control of coupling properties and energy transfer (ET) between the QDs is desired to enhance efficiency and performance.[16]

ET in QD solids was studied in several previous works. These include layered QD solids realized by the Langmuir−Blodgett/spin-coating techniques,[17−19] by electrostatic layer-by-layer self-assembly,[20−22] or by using dithiol linkers.[16,23,24] ET rates as high as 71 $ps^{-1}$ were reported in layers of donor and acceptor QDs in close proximity,[20] with a rate of 50 $ps^{-1}$ derived for a specific subspecies within the ensemble inhomogeneous distribution. In many of the works, it has been pointed out that the ET for the case of close-packed QDs deviates from the basic perturbation regime of the dipole−dipole interactions that lead to the known Förster resonance energy transfer (FRET) mechanism.[18,21,22,25−27] Yet, no clear attempt was made to achieve control over coupling properties and to comprehensively study the effect of QD linkers upon ET.

Here, we use dithiol-linking molecules to realize bi-size QD solids. The sizes of the QDs are such that the first excitonic state of the smaller dot is quasi-resonant with the second exciton of the larger dot. Using ultrafast transient absorption (TA) spectroscopy, the fast ET between donor and acceptor QDs is examined. By alternating between different lengths of the linking molecule, we aim to control the QDs' coupling strength and ET rates. The measured rates and their dependence on the length of the linker molecules point to a coherent contribution to the ET dynamics beyond the perturbative regime.

## EXPERIMENTAL SECTION

**Sample Preparation.** Colloidal CdSe QDs were synthesized according to Lifshitz et al.[28] QDs of two different sizes were used: smaller QDs with a mean diameter of around 2.75 nm (QDs A) or larger ones with a mean diameter of 3.45 nm(QDs B). A disordered structure of covalently bonded QDs was realized using wet chemistry, as described in detail in our prior publications.[5,29] Samples were composed of either one size QDs or both sizes of QDs to examine ET between small and large QDs (as schematically shown in Figure 1c,d, respectively). We used alkanedithiol molecules, of two different

**Received:** November 30, 2017
**Revised:** January 21, 2018
**Published:** February 12, 2018





DOI: 10.1021/acs.jpcc.7b11799
J. Phys. Chem. C XXXX, XXX, XXX−XXX

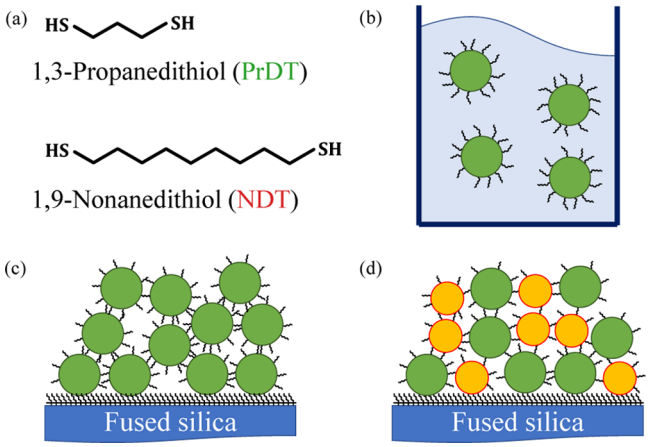


**Figure 1.** (a) Chemical structure of the alkanedithiol linker molecules used in present work. (b–d) Schematic illustrations of QD samples under investigation: (b) QDs in solution (isolated). (c) Single-size QD disordered structures. (d) Disordered structure of QDs of two sizes.

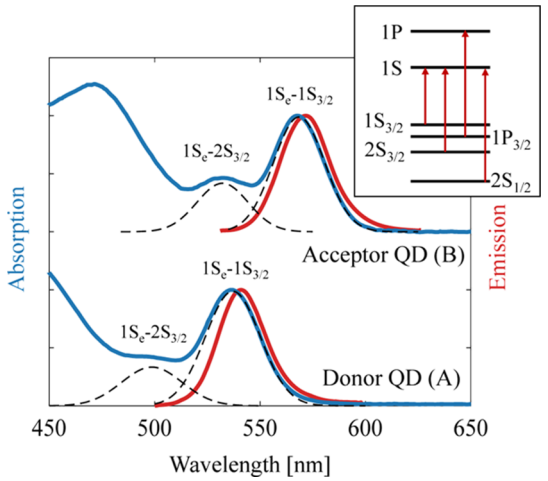


**Figure 2.** Steady-state absorption (in blue) and emission (in red) of the 2.75 nm QDs (bottom) and 3.45 nm QDs (top) in toluene solution. The thin dashed lines represent Gaussian fits for the first two bands in the absorption spectra. The smaller QDs A exhibit a lowest unoccupied molecular orbital $1S_e-1S_{3/2}$ level resonant with the $1S_e-2S_{3/2}$ level of the bigger QDs B. The inset displays the excitonic energy structure of the dots, with first few electron and hole states, and the allowed transitions between them.

lengths, as linkers between dots (Figure 1a). The molecules, presented in Figure 1a, are the shorter 1,3-propanedithiol (PrDT) and the longer 1,9-nonanedithiol (NDT), with nominal lengths of 5.5 and 13 Å, respectively. They form covalent bonds with QD Cd atoms at both ends.[30,31] QDs in original toluene solution were measured as well, as a reference of isolated, noncoupled dots. Consecutive dipping of fused silica substrates in QD solution and linking molecule solution and repeating the process for ~30 times yielded a disordered layered structure, as Figure 1c,d illustrates. The adsorption procedure was carried out under a dry nitrogen environment, and consecutive sealing of the sample was done for their encapsulation and prevention of oxidization. It should be noted that the adsorption procedure, which leads to a rather disordered structure, was used to obtain a three-dimensional, isotropic structure, with clear signatures of ET. This was done to prevent a preferred ET direction. Yet, it can easily be modified to provide a cascaded bi-layer or multi-layer structure of size-gradient QDs, as proposed before.[32]

**Experimental Methods.** A home-built ultrafast TA (pump-probe) setup was used to investigate electronic dynamics of the samples. A detailed description of the setup and measurement procedures is found in the Supporting Information. Pump pulses (400 nm) were used to excite the samples, followed by a white-light probe pulse. At this excitation wavelength, QDs of both sizes are excited. Very low power pump pulses were used to achieve a low average number of excitons per dot, $\langle N_{ex} \rangle \ll 1$. This was done to avoid multiexciton generation in a single dot and minimize the effect of excited neighboring dots.

## RESULTS AND DISCUSSION

Figure 2 shows steady-state absorption spectra of the two types of QDs used in toluene solution. The smaller QDs A exhibit a band edge absorption peak at 537 nm, whereas the bigger QDs B has their band-edge absorption peak at 567 nm. The first few energy levels are clearly visible in the spectra, and a Gaussian fit for the two lowest states appears in the figure as well. These two levels correspond to the electron–hole pair $1S_e-1S_{3/2}$ and $1S_e-2S_{3/2}$ states. From the spectra, it is possible to see that the small QD band-edge energy level (1S) is resonant with the 2S energy level of the bigger QDs. Steady-state absorption measurements of the adsorbed samples suffer from a high degree of scattering, thereby yielding results of poor quality. Trends such as red shift of the absorption bands are clearly seen, yet quantitatively measuring the coupling strength is not realistic by such steady-state measurements.

Ultrafast TA measurements were conducted on all different samples, allowing us to follow the dynamics of the system and to overcome scattering issues. Figure 3 compares results for three of these samples; absorption difference ($\Delta A$) for different pump-probe delay times, ranging from 0 to 500 ps, is shown for QDs B in all three configurations—in toluene solution (noncoupled) and in a layered structure with NDT and PrDT linker molecules. The two negative dips which are marked $B_1$ and $B_2$ in Figure 3a originate from the ground state bleach (GSB) of the 1S and 2S states. Relaxation of the hot charge carriers to the lowest energetic levels occurs within a timescale of hundreds of fs[33,34] and is followed by slower radiative and nonradiative transitions of the electron–hole pair to the ground state. At both ends of the displayed spectrum, two photoinduced absorption signals appear, labeled $A_1$ and $A_2$. These can be assigned to bi-excitonic processes.[33,35] Within a few ps timescale, only relatively small changes in the spectra shape are visible, as the dominant process observed in this system is the longer ns-timescale decay of the signal.

Nevertheless, clear differences are easily identified among the TA spectrum of the three samples. The transition from noncoupled QDs to coupled QDs appears with a shift of the $B_1$ and $B_2$ levels to lower energies. Table 1 presents the position of these two bands for all samples for a pump-probe delay time of $\Delta t$ = 10 ps, and the coupled QDs energy bands shift relative to the noncoupled band position. The position was determined using Gaussian fits for the peaks. The coupled QDs exhibit a red shift of the 1S level, of about 8 meV for the long NDT linkers, and about 18 meV for the short PrDT linkers. We attribute this red shift, which is accompanied by small broadening of the bands as well, to the coupling (within weak-coupling regime) of the QD energy levels with neighboring dots. The 2S level, having a less localized nature,


DOI: 10.1021/acs.jpcc.7b11799
J. Phys. Chem. C XXXX, XXX, XXX–XXX

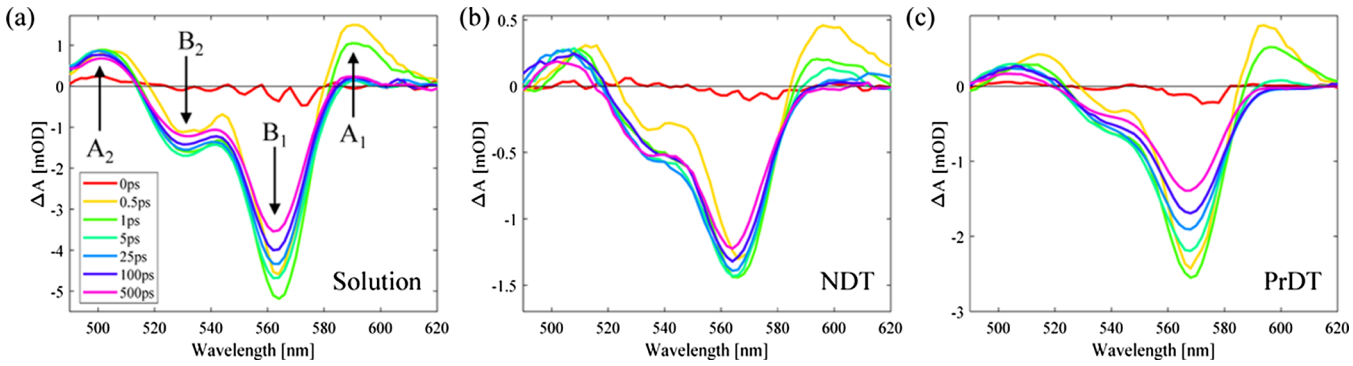


**Figure 3.** TA spectrum for different pump-probe delay times for QDs B in (a) solution (isolated), (b) linked with NDT (longer linker), and (c) linked with PrDT (shorter linker).

**Table 1. Position of the $B_1$ and $B_2$ Bands at Delay Time $\Delta t$ = 10 ps for QDs B in Solution and Linked with NDT and PrDT, Including Their Relative Energetic Shift from Bands in Solution**[a]

| | solution | NDT | | PrDT | |
|---|---|---|---|---|---|
| energy level | position (nm) | position (nm) | shift (meV) | position (nm) | shift (meV) |
| $1S-1S_{3/2}$ ($B_1$) | 562.9 | 565 | 8.2 | 567.5 | 17.9 |
| $1S-2S_{3/2}$ ($B_2$) | 531.4 | 537.7 | 27.3 | 540.4 | 38.9 |

[a]Estimated error is <±0.5 nm in wavelength or 3 meV in energy.

is coupled even stronger, yielding a shift that is larger by ~20 meV for both linkers. The smaller QDs A exhibited an even stronger effect pronounced as a red shift doubled in energy (see the Supporting Information). The effect of the linker molecule on coupling properties and delocalization of the wavefunction has also been the subject of our previous published work.[5,29] As we have previously shown,[5] these observed signatures in the TA signal cannot be fully explained as rising due to trapping of excitons at newly created surface states. Also, it should be emphasized that the two ends of the linking molecules have the same head group (a thiol), and therefore, there should be no difference in surface-related effects between the two linked dots.

Combining QDs of the two sizes in our samples allows us to trace existence and rate of excitonic energy transfer (EET) among neighboring QDs via a dipole−dipole mechanism. This is done by tracing the TA signal decay at probe wavelengths corresponding the two QDs $B_1$ bands. Figure 4a presents the ratio of $\Delta A$ at around 537 nm (B1 of QDs A and B2 of QDs B) and $\Delta A$ at around 567 nm (B1 of QDs B) as a function of time for samples including only QDs B and those incorporating both QDs A and QDs B. They are normalized to 1 at 600 fs after both the contributions from coherent artifacts and intraband transitions die out. The three samples containing QDs B only are presented by dashed lines; they all show roughly the same dynamics. In solid lines, the samples of both QD sizes appear. Here, differences between the three samples are clear. The expected qualitative trends for EET in coupled samples between donor QDs A and acceptor QDs B are clearly seen. The effect is more dominant and faster when the shorter PrDT linkers are used. It should be pointed out that the TA signals at the mentioned probe wavelengths are not necessarily proportional to the 1S/2S state population. QDs B mainly exhibit a GSB of $B_2$ and $B_1$ bands at the probing wavelengths of 537 and

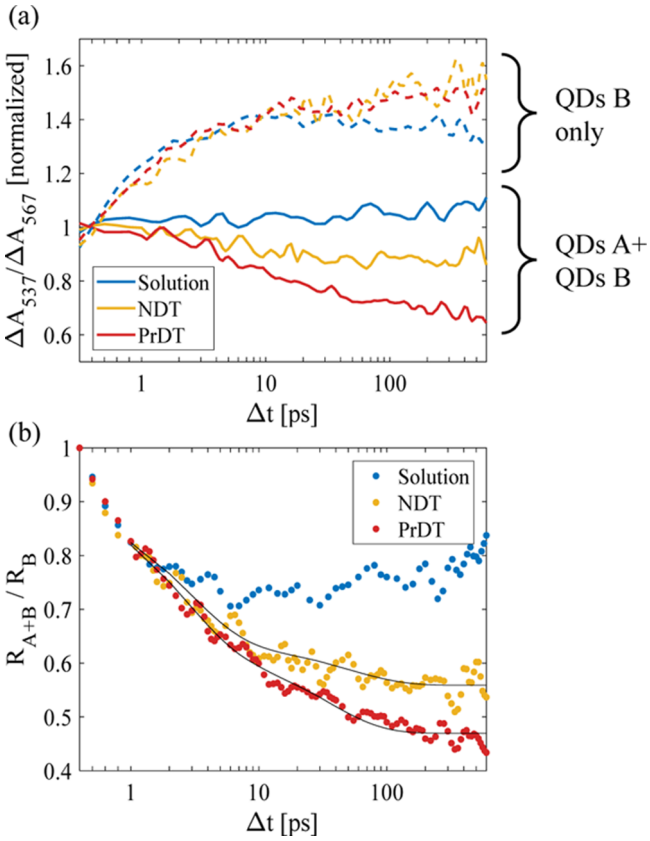


**Figure 4.** (a) Ratios of the TA $\Delta A$ signal probed at the small QD band edge (537 nm) with that probed at the big QD band edge (567 nm) for noncoupled dots in solution (blue) and for coupled QDs linked with NDT (yellow) and with PrDT (red) as a function of the pump-probe delay time. The dashed lines present samples with big QDs only (QDs B), and the solid lines represent samples incorporating both small and big QDs (donor−acceptor systems). (b) Ratios of $\Delta A_{537}/\Delta A_{567}$ from Figure 4a of donor−acceptor systems (QDs A + QDs B) with those of acceptor systems only (QDs B). The black lines represent three components fits, as described in the main text. All plots are normalized to 1 at a delay time of 600 fs.

567 nm, respectively (see Figure 3); QDs A have their $B_1$ and $A_1$ features at these wavelengths. To obtain a quantitative value for the EET rate, we have divided the ratio of $\Delta A_{537}/\Delta A_{567}$ for the QDs A + QDs B samples with that of the QDs B only when the last acts as a reference baseline. The results are shown in Figure 4b. The plots present three components with three timescales that can be fitted to a relation of the form $f(t) = a_1$



DOI: 10.1021/acs.jpcc.7b11799
J. Phys. Chem. C XXXX, XXX, XXX−XXX

$\exp(-t/\tau_1) + a_2 \exp(-t/\tau_2) + c$, as presented for the NDT- and PrDT-linked samples in Figure 4b (solid black lines).

For very short times of up to few ps, all samples show dynamics quite independent of coupling properties. On such timescales, dynamics is governed by intradot transitions, as was already manifested in our previous publication.[5] The mild changes that do exist can be ascribed to surface effects rather than interdot effects. The adsorption process of the QDs in the layered structures (i.e., the NDT and PrDT-linked) includes an exchange of their original ODA ligands with thiol molecules. This can, for example, alter passivation of surface traps, allowing fast trapping of charge carriers. Such effects should have approximately the same influence on both NDT- and PrDT-linked samples, as both share the same thiol linking head group. Indeed, the first time scale $\tau_1$ for both has the same value of ∼3 ps, matching previous reports.[36,37] The QDs in solution are probably better passivated, and so, they present a more modest decay during that timescale.

The second time scale corresponds to the EET rate from the donor QDs A to the acceptor QDs B. It is found to be 50 $ps^{-1}$ for the NDT and 30 $ps^{-1}$ for the PrDT. A relatively large error range is associated with these values, as they varied according to the fitting procedure; an error factor of up to 1.5 is plausible. That said, these are among the fastest EET rates achieved in coupled QDs. We will address this shortly.

Lastly, at the third time scale, the recombination of the electron−hole pair is the dominant process. As this takes place in ns time scales,[38,39] it can be regarded as a constant within our measurement time frame ($c$, in the abovementioned fit equation).

We believe that the very fast EET between the dots was accomplished by proper selection of the QDs and the linking molecules. By maximizing the overlap between the donor QD emission spectrum and the 2S band absorption of the acceptor QDs (see Figure 2), EET rate is increased,[17,23] as it is directly linked to the overlap integral between the two.[40,41] Once energy is transferred to the 2S band of the acceptor QDs B, a very fast intraband decay to the 1S levels occurs in a matter of hundreds of fs.[34] Moreover, because of the quasi-resonance condition between the excited states of dots of different sizes, delocalization of excitons on QD dimers may speed up the transfer process, as we will discuss further below.

The linking molecules have few roles in controlling the detected coupling properties. The first and most pronounced is determining the interdot spacing. The center-to-center distance of adjacent QDs of the type A and B is 3.65 nm for the PrDT-linked dots and 4.4 nm for the NDT-linked ones. It is well-known that FRET rates obey a $1/R^6$ dependency with respect to the donor−acceptor distance, $R$. Bearing in mind the large uncertainty in the ET rates, and having only two different distances, our results still seemingly present a large deviation from this power law. Yet, deviations from the classical case of the point-dipole donor−acceptor case have already been witnessed and discussed before.[21,22,26,27] Our results better fit a $\sim 1/R^3$ ET rate dependency. Such dependency is expected in a case of the bulk acceptor,[42,43] which might describe our three-dimensional structure of QDs. Yet, while this form of incoherent ET is possible in our system, the disordered nature of our system makes it more improbable. Another mechanism of coherent ET between dimers is more likely, as described by our theoretical model suggested below.

Second, the linking molecules form covalent bonds with the Cd atoms of the QDs at both ends.[30,31] We believe that this type of bridging between QDs—in comparison with the electrostatic or physical forces involved in Langmuir−Blodgett layer-by-layer methods methods for QD film preparation—is more efficient in terms of charge/exciton transfer. Coherent charge transfer was shown to be small for alkyl dithiols linkers.[5,44] Single-molecule transport measurements show up to three orders of magnitude better conductivity for chemically bonded contacts in respect to nonbonded ones.[45,46] For photoexcitation, ET is also expected to be more efficient because it is closely related to the size of the excitonic wavefunction; covalent bonds at the surface of the QD lower the charge carriers confinement, therefore yielding less localized excitons. We have addressed this issue in a previous publication.[5]

To provide a clear and simple illustration of the coupling mechanism between the photoexcited donor and acceptor QDs in our system, a theoretical model was established. The model is described in detail in the Supporting Information. The coupling that results from quasi-resonance that is engineered between the $1S_e-2S_{3/2}$ transition of the acceptor and the $1S_e-1S_{3/2}$ transition of the donor creates a state delocalized over the two dots. In the limiting case of an exact resonance, the ET rate scales as $1/R^3$, with calculated transfer rates that compare well with the experimentally measured timescales shown in Figure 4b. The calculated transfer rates for the resonance case are plotted in Figure 5 as a function of the center-to-center distance between donor and acceptor dots. The radius of each dot is adjusted to agree with the experimentally measured transition frequencies, as calculated by our simplistic model, hence the deviation from the actual values (see the Supporting Information). These results suggest the existence of a fast, coherent dipole−dipole interaction between the QD excitons for the dimers that are resonant. For those that are out of resonance, the coupling falls in the perturbative regime which leads to slower ET rates, which is in agreement with the Förster regime.

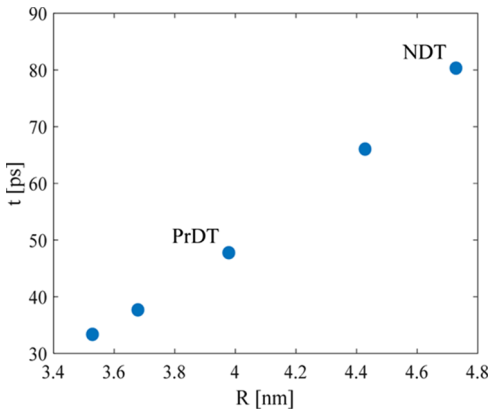


**Figure 5.** Calculated time necessary for a complete transfer of population from the donor dot to the acceptor dot in the resonance condition as a function of center-to-center dot separation. The center-to-center distances ($R$) correspond to surface-to-surface distances of 1, 2.5, 5.5, 10, and 13 Å.

## CONCLUSIONS

In this work, we studied the photoinduced ET in disordered multi-layered structures of coupled QDs. We have demonstrated a very fast ET in an optimally tuned donor−acceptor



DOI: 10.1021/acs.jpcc.7b11799
J. Phys. Chem. C XXXX, XXX, XXX−XXX

system, with rates as high as 30 $ps^{-1}$. These rates show dependency in the donor−acceptor distance, which is controlled by the incorporation of dithiol linkers. The dependency greatly deviates from the one expected from a dipole−dipole FRET mechanism, suggesting the existence of a coherent dipole−dipole interaction, made dominant by the quasi-resonance condition that was engineered by tuning the donor−acceptor system. We attribute the fast ET rates, in part, to the outcome of the covalent bonds between the QDs and the linking molecules. As we have shown earlier as well,[5] the excitonic wavefunction tends to delocalize outside the single QD in the presence of such bonds, leading to better coupling properties with neighboring dots. With this work, we present the ability to further control and enhance ET in QD solids, for tailored applicative uses at ambient conditions ranging from solar energy harvesting to LEDs and lasing, where the rate of ET is critical, as it competes with disorder and fast quenching.

## ■ ASSOCIATED CONTENT

### Supporting Information

The Supporting Information is available free of charge on the ACS Publications website at DOI: 10.1021/acs.jpcc.7b11799.

Transient absorption setup, additional data, and theoretical energy transfer model (PDF)

## ■ AUTHOR INFORMATION


### Corresponding Author

*E-mail: paltiel@mail.huji.ac.il.

### ORCID

Eyal Cohen: 0000-0003-0457-9200

Francoise Remacle: 0000-0001-7434-5245

Barbara Fresch: 0000-0002-0988-0644


### Author Contributions

The manuscript was written through contributions of all authors. All authors have given approval to the final version of the manuscript.

### Notes

The authors declare no competing financial interest.

## ■ ACKNOWLEDGMENTS

This work was supported by the European Commission via the Marie-Sklodowska Curie action Phonsi (H2020-MSCA-ITN-642656) and the Wolfson Foundation. We acknowledge the support of the H2020 FET open project COPAC 766563. FR acknowledges the support of the Fonds National de la Recherche Scientifique, FRS-FNRS, Belgium. BF acknowledges the support of the Italian Ministero dell'Istruzione, Università e Ricerca through the grant Rita Levi Montalcini (2013).

## ■ REFERENCES


(1) Murray, C. B.; Kagan, C. R.; Bawendi, M. G. Self-Organization of CdSe Nanocrystallites into Three-Dimensional Quantum Dot Superlattices. *Science* **1995**, *270*, 5240.

(2) Tour, J. M. Molecular Electronics. Synthesis and Testing of Components. *Acc. Chem. Res.* **2000**, *33*, 791−804.

(3) Nitzan, A.; Ratner, M. A. Electron Transport in Molecular Wire Junctions. *Science* **2003**, *300*, 1384−1389.

(4) National Academy of Engineering. *Frontiers of Engineering: Reports on Leading-Edge Engineering from the 2003 NAE Symposium on Frontiers of Engineering*; National Academies Press, 2004.

(5) Cohen, E.; Gdor, I.; Romero, E.; Yochelis, S.; van Grondelle, R.; Paltiel, Y. Achieving Exciton Delocalization in Quantum Dot Aggregates Using Organic Linker Molecules. *J. Phys. Chem. Lett.* **2017**, *8*, 1014−1018.

(6) Colvin, V. L.; Goldstein, A. N.; Allivisatos, A. P.; Alivisatos, A. P. Semiconductor Nanocrystals Covalently Bound to Metal Surfaces with Self-Assembled Monolayers. *J. Am. Chem. Soc.* **1992**, *114*, 5221−5230.

(7) Colvin, V. L.; Schlamp, M. C.; Alivisatos, A. P. Light-Emitting Diodes Made from Cadmium Selenide Nanocrystals and a Semiconducting Polymer. *Nature* **1994**, *370*, 354−357.

(8) Sun, L.; Choi, J. J.; Stachnik, D.; Bartnik, A. C.; Hyun, B.-R.; Malliaras, G. G.; Hanrath, T.; Wise, F. W. Bright Infrared Quantum-Dot Light-Emitting Diodes through Inter-Dot Spacing Control. *Nat. Nanotechnol.* **2012**, *7*, 369.

(9) Tang, J.; Kemp, K. W.; Hoogland, S.; Jeong, K. S.; Liu, H.; Levina, L.; Furukawa, M.; Wang, X.; Debnath, R.; Cha, D.; et al. Colloidal-Quantum-Dot Photovoltaics Using Atomic-Ligand Passivation. *Nat. Mater.* **2011**, *10*, 765.

(10) Hanrath, T. Colloidal Nanocrystal Quantum Dot Assemblies as Artificial Solids. *J. Vac. Sci. Technol., A* **2012**, *30*, 030802.

(11) Choi, J.-H.; Fafarman, A. T.; Oh, S. J.; Ko, D.-K.; Kim, D. K.; Diroll, B. T.; Muramoto, S.; Gillen, J. G.; Murray, C. B.; Kagan, C. R. Bandlike Transport in Strongly Coupled and Doped Quantum Dot Solids: A Route to High-Performance Thin-Film Electronics. *Nano Lett.* **2012**, *12*, 2631−2638.

(12) Talgorn, E.; Gao, Y.; Aerts, M.; Kunneman, L. T.; Schins, J. M.; Savenije, T. J.; van Huis, M. A.; van der Zant, H. S. J.; Houtepen, A. J.; Siebbeles, L. D. A. Unity Quantum Yield of Photogenerated Charges and Band-like Transport in Quantum-Dot Solids. *Nat. Nanotechnol.* **2011**, *6*, 733−739.

(13) Li, X.; Wu, Y.; Steel, D.; Gammon, D.; Stievater, T. H.; Katzer, D. S.; Park, D.; Piermarocchi, C.; Sham, L. J. An All-Optical Quantum Gate in a Semiconductor Quantum Dot. *Science* **2003**, *301*, 809−811.

(14) Remacle, F.; Heath, J. R.; Levine, R. D. Electrical Addressing of Confined Quantum Systems for Quasiclassical Computation and Finite State Logic Machines. *Proc. Natl. Acad. Sci. U.S.A.* **2005**, *102*, 5653−5658.

(15) Fresch, B.; Hiluf, D.; Collini, E.; Levine, R. D.; Remacle, F. Molecular Decision Trees Realized by Ultrafast Electronic Spectroscopy. *Proc. Natl. Acad. Sci. U.S.A.* **2013**, *110*, 17183−17188.

(16) Crooker, S. A.; Hollingsworth, J. A.; Tretiak, S.; Klimov, V. I. Spectrally Resolved Dynamics of Energy Transfer in Quantum-Dot Assemblies: Towards Engineered Energy Flows in Artificial Materials. *Phys. Rev. Lett.* **2002**, *89*, 186802.

(17) Achermann, M.; Petruska, M. A.; Crooker, S. A.; Klimov, V. I. Picosecond Energy Transfer in Quantum Dot Langmuir−Blodgett Nanoassemblies. *J. Phys. Chem. B* **2003**, *107*, 13782−13787.

(18) Zheng, K.; Žídek, K.; Abdellah, M.; Zhu, N.; Chábera, P.; Lenngren, N.; Chi, Q.; Pullerits, T. Directed Energy Transfer in Films of CdSe Quantum Dots: Beyond the Point Dipole Approximation. *J. Am. Chem. Soc.* **2014**, *136*, 6259−6268.

(19) Akselrod, G. M.; Prins, F.; Poulikakos, L. V.; Lee, E. M. Y.; Weidman, M. C.; Mork, A. J.; Willard, A. P.; Bulović, V.; Tisdale, W. A. Subdiffusive Exciton Transport in Quantum Dot Solids. *Nano Lett.* **2014**, *14*, 3556−3562.

(20) Franzl, T.; Shavel, A.; Rogach, A. L.; Gaponik, N.; Klar, T. A.; Eychmüller, A.; Feldmann, J. High-Rate Unidirectional Energy Transfer in Directly Assembled CdTe Nanocrystal Bilayers. *Small* **2005**, *1*, 392−395.

(21) Kim, D.; Okahara, S.; Nakayama, M.; Shim, Y. Experimental Verification of Förster Energy Transfer between Semiconductor Quantum Dots. *Phys. Rev. B: Condens. Matter Mater. Phys.* **2008**, *78*, 153301.

(22) Kholmicheva, N.; Moroz, P.; Bastola, E.; Razgoniaeva, N.; Bocanegra, J.; Shaughnessy, M.; Porach, Z.; Khon, D.; Zamkov, M. Mapping the Exciton Diffusion in Semiconductor Nanocrystal Solids. *ACS Nano* **2015**, *9*, 2926−2937.

(23) Xu, F.; Ma, X.; Haughn, C. R.; Benavides, J.; Doty, M. F.; Cloutier, S. G. Efficient Exciton Funneling in Cascaded PbS Quantum Dot Superstructures. *ACS Nano* **2011**, *5*, 9950−9957.




DOI: 10.1021/acs.jpcc.7b11799
J. Phys. Chem. C XXXX, XXX, XXX−XXX

(24) Zhang, J.; Tolentino, J.; Smith, E. R.; Zhang, J.; Beard, M. C.; Nozik, A. J.; Law, M.; Johnson, J. C. Carrier Transport in PbS and PbSe QD Films Measured by Photoluminescence Quenching. *J. Phys. Chem. C* **2014**, *118*, 16228−16235.
(25) Allan, G.; Delerue, C. Energy Transfer between Semiconductor Nanocrystals: Validity of Förster's Theory. *Phys. Rev. B: Condens. Matter Mater. Phys.* **2007**, *75*, 195311.
(26) Baer, R.; Rabani, E. Theory of Resonance Energy Transfer Involving Nanocrystals: The Role of High Multipoles. *J. Chem. Phys.* **2008**, *128*, 184710.
(27) Mork, A. J.; Weidman, M. C.; Prins, F.; Tisdale, W. A. Magnitude of the Förster Radius in Colloidal Quantum Dot Solids. *J. Phys. Chem. C* **2014**, *118*, 13920−13928.
(28) Grumbach, N.; Capek, R. K.; Tilchin, E.; Rubin-Brusilovski, A.; Yang, J.; Ein-Eli, Y.; Lifshitz, E. Comprehensive Route to the Formation of Alloy Interface in Core/Shell Colloidal Quantum Dots. *J. Phys. Chem. C* **2015**, *119*, 12749−12756.
(29) Cohen, E.; Gruber, M.; Romero, E.; Yochelis, S.; van Grondelle, R.; Paltiel, Y. Properties of Self-Assembled Hybrid Organic Molecule/Quantum Dot Multilayered Structures. *J. Phys. Chem. C* **2014**, *118*, 25725−25730.
(30) Dance, I. G.; Choy, A.; Scudder, M. L. Syntheses, Properties, and Molecular and Crystal Structures of (Me4N)4[E4M10(SPh)16] (E = Sulfur or Selenium; M = Zinc or Cadmium): Molecular Supertetrahedral Fragments of the Cubic Metal Chalcogenide Lattice. *J. Am. Chem. Soc.* **1984**, *106*, 6285−6295.
(31) Qu, L.; Peng, Z. A.; Peng, X. Alternative Routes toward High Quality CdSe Nanocrystals. *Nano Lett.* **2001**, *1*, 333−337.
(32) Klar, T. A.; Franzl, T.; Rogach, A. L.; Feldmann, J. Super-Efficient Exciton Funneling in Layer-by-Layer Semiconductor Nanocrystal Structures. *Adv. Mater.* **2005**, *17*, 769−773.
(33) Klimov, V. I. Optical Nonlinearities and Ultrafast Carrier Dynamics in Semiconductor Nanocrystals. *J. Phys. Chem. B* **2000**, *104*, 6112−6123.
(34) Kambhampati, P. Hot Exciton Relaxation Dynamics in Semiconductor Quantum Dots: Radiationless Transitions on the Nanoscale. *J. Phys. Chem. C* **2011**, *115*, 22089−22109.
(35) Klimov, V.; Hunsche, S.; Kurz, H. Biexciton Effects in Femtosecond Nonlinear Transmission of Semiconductor Quantum Dots. *Phys. Rev. B: Condens. Matter Mater. Phys.* **1994**, *50*, 8110−8113.
(36) Zhang, X.; Izutsu, M. Ultrafast Processes of Highly Excited Carriers in CdS X Se 1-X -Doped Glass. *Jpn. J. Appl. Phys.* **1998**, *37*, 6025−6028.
(37) Garrett, M. D.; Dukes, A. D., III; McBride, J. R.; Smith, N. J.; Pennycook, S. J.; Rosenthal, S. J. Band Edge Recombination in CdSe, CdS and CdS X Se 1−X Alloy Nanocrystals Observed by Ultrafast Fluorescence Upconversion: The Effect of Surface Trap States. *J. Phys. Chem. C* **2008**, *112*, 12736−12746.
(38) *Nanocrystal Quantum Dots*, 2nd ed.; Klimov, V. I., Ed.; CRC Press, 2010.
(39) Liu, I.-S.; Lo, H.-H.; Chien, C.-T.; Lin, Y.-Y.; Chen, C.-W.; Chen, Y.-F.; Su, W.-F.; Liou, S.-C. Enhancing Photoluminescence Quenching and Photoelectric Properties of CdSe Quantum Dots with Hole Accepting Ligands. *J. Mater. Chem.* **2008**, *18*, 675.
(40) Forster, T. Intermolecular Energy Migration and Fluorecence. *Ann. Phys.* **1948**, *2*, 55 DOI: 10.1002/andp.19484370105.
(41) Lakowicz, J. R. *Principles of Fluorescence Spectroscopy*; Springer, 2006.
(42) Rogach, A. L.; Klar, T. A.; Lupton, J. M.; Meijerink, A.; Feldmann, J. Energy Transfer with Semiconductor Nanocrystals. *J. Mater. Chem.* **2009**, *19*, 1208.
(43) Kundu, S.; Patra, A. Nanoscale Strategies for Light Harvesting. *Chem. Rev.* **2017**, *117*, 712−757.
(44) Wang, H.; McNellis, E. R.; Kinge, S.; Bonn, M.; Cánovas, E. Tuning Electron Transfer Rates through Molecular Bridges in Quantum Dot Sensitized Oxides. *Nano Lett.* **2013**, *13*, 5311−5315.
(45) Cui, X. D.; Primak, A.; Zarate, X.; Tomfohr, J.; Sankey, O. F.; Moore, A. L.; Moore, T. A.; Gust, D.; Harris, G.; Lindsay, S. M. Reproducible Measurement of Single-Molecule Conductivity. *Science* **2001**, *294*, 5542.
(46) Salomon, A.; Cahen, D.; Lindsay, S.; Tomfohr, J.; Engelkes, V. B.; Frisbie, C. D. Comparison of Electronic Transport Measurements on Organic Molecules. *Adv. Mater.* **2003**, *15*, 1881−1890.


DOI: 10.1021/acs.jpcc.7b11799
J. Phys. Chem. C XXXX, XXX, XXX−XXX